SCIENCE CHINA
Chemistry

• ARTICLES •
• SPECIAL TOPIC • Bio-based and Biodegradable Polymers

November 2016 Vol.59 No.11: 1405–1414
doi: 10.1007/s11426-016-0205-5

Light weight, mechanically strong and biocompatible α-chitin aerogels from different aqueous alkali hydroxide/urea solutions

Beibei Ding[1,4†], Dan Zhao[1†], Jianhui Song[2], Huichang Gao[3], Duoduo Xu[1], Min Xu[2], Xiaodong Cao[3], Lina Zhang[1] & Jie Cai[1*]

[1]*College of Chemistry & Molecular Sciences, Wuhan University, Wuhan 430072, China*
[2]*Department of Physics, Shanghai Key Laboratory of Magnetic Resonance, East China Normal University, Shanghai 200062, China*
[3]*School of Materials Science and Engineering, South China University of Technology, Guangzhou 510641, China*
[4]*Key Laboratory of Rubber-Plastics, Ministry of Education; Shandong Provincial Key Laboratory of Rubber-Plastics, Qingdao University of Science & Technology, Qingdao 266042, China*

Received May 4, 2016; accepted July 3, 2016; published online October 9, 2016

Light weight and mechanically strong α-chitin aerogels were fabricated using the sol-gel/self-assembly method from α-chitin in different aqueous alkali hydroxide (KOH, NaOH and LiOH)/urea solutions. All of the α-chitin solutions exhibited temperature-induced rapid gelation behavior. ^{13}C nuclear magnetic resonance (NMR) spectra revealed that the aqueous alkali hydroxide/urea solutions are non-derivatizing solvents for α-chitin. Fourier transform infrared (FT-IR), X-ray diffraction (XRD) and cross-polarization magic angle spinning (CP/MAS) ^{13}C NMR confirmed that α-chitin has a stable aggregate structure after undergoing dissolution and regeneration. Subsequently, nanostructured α-chitin aerogels were fabricated by regeneration from the chitin solutions in ethanol and then freeze-drying from *t*-BuOH. These α-chitin aerogels exhibited high porosity (87% to 94%), low density (0.09 to 0.19 g/cm^3), high specific surface area (419 to 535 m^2/g) and large pore volume (2.7 to 3.8 cm^3/g). Moreover, the α-chitin aerogels exhibited good mechanical properties under compression and tension models. *In vitro* studies showed that mBMSCs cultured on chitin hydrogels have good biocompatibility. These nanostructured α-chitin aerogels may be useful for various applications, such as catalyst supports, carbon aerogel precursors and biomedical materials.

chitin, aerogels, alkali hydroxide/urea aqueous solutions, mechanical properties, biocompatibility

Citation: Ding B, Zhao D, Song J, Gao H, Xu D, Xu M, Cao X, Zhang L, Cai J. Light weight, mechanically strong and biocompatible α-chitin aerogels from different aqueous alkali hydroxide/urea solutions. *Sci China Chem*, 2016, 59: 1405−1414, doi: 10.1007/s11426-016-0205-5

1 Introduction

Biomacromolecules, such as cellulose, chitin, chitosan, alginate, collagen and gelatin, have been investigated because of their inherent hydrophilicity, biocompatibility and biodegradability [1–8]. One biomacromolecule, chitin, is composed of β-(1,4)-linked chains of *N*-acetyl-*D*-glucosamine and is the second-most abundant natural polysaccharide; chitin exists in arthropods' exoskeletons and the cell walls of fungi and yeast and consists of ordered crystalline nanofibrils that form a hierarchical structure [4,9–11]. The rigid and close-packed chitin chains are involved in numerous intra- and inter-molecular hydrogen bonds, which make chitin difficult to dissolve.

Several solvents, such as lithium chloride/tertiary amides (dimethylformamide, *N*,*N*-dimethylacetamide and *N*-methyl-2-pyrrolidone) [9], concentrated acids (HCl, methane sulfonic acid, dichloroacetic and trichloroacetic acids) [12], aqueous NaOH [13–15], calcium chloride dihydrate-satur-

†These authors contributed equally to this work.
*Corresponding author (email: caijie@whu.edu.cn)

ated methanol [16], saturated lithium thiocyanate [17], fluorinated alcohols (hexafluoro-2-propanol and hexafluoroacetone sesquihydrate) [18], ionic liquids (1-butyl-3-methylimidazolium acetate, 1-ethyl-3-methyl-imidazolium acetate and 1-allyl-3-methylimidazolium bromated) [19–21], and deep eutectic solvents (choline halide/urea or thiourea) [22,23], have been used to dissolve chitin. Alternatively, nanostructured biomaterials can offer environments that mimic the extracellular matrix for cell growth [24–28]. However, the exploitation of nanostructured chitin hydrogels and aerogels is hampered by their low solubility in common solvents, poor mechanical integrity, and difficult fabrication.

Ten years ago, we developed a novel solvent system for the rapid dissolution of cellulose in precooled LiOH/urea and NaOH/urea aqueous solutions [29]. Subsequently, chitin and chitosan were successfully dissolved in NaOH/urea and LiOH/urea aqueous solutions, respectively, by freeze-thawing cycle processes [30–32]. Recently, we used an optimized aqueous solution (11 wt% NaOH/4 wt% urea) to prepare a concentrated chitin solution and fabricate chitin aerogels, sponges, fibers, and microspheres [33–37]. Interestingly, we also found that chitin is soluble in KOH/urea aqueous solution, which could only slightly dissolve cellulose and had never been reported to dissolve chitin [38].

Here, we present preliminary but remarkable results demonstrating the rheological behavior of the α-chitin solutions in aqueous alkali hydroxide (KOH, NaOH and LiOH)/urea solutions and describe the structure and properties of the nanostructured α-chitin hydrogels and aerogels to provide meaningful information supporting the search for new solvents for aqueous chitin systems and the development of novel chitin nanomaterials. The formation of the α-chitin hydrogels involves the regeneration of homogenous aqueous α-chitin/alkali hydroxide/urea solutions through physical gelation with ethanol, followed by thorough washing with deionized water. The resulting α-chitin hydrogels were freeze-dried from *t*-BuOH to give aerogels with low-density (0.09–0.17 g/cm^3), large surface area (up to 535 m^2/g) and good mechanical properties for various potential applications, including as catalyst supports, carbon aerogel precursors and biomedical materials.

2 Experimental

2.1 Materials

The raw α-chitin powder was purchased from Golden-Shell Biochemical Co. Ltd. (China). The α-chitin was purified according to our previous work [33]. The raw α-chitin powder was treated with 1 M NaOH aqueous solution at ambient temperature overnight, then 0.3% $NaClO_2$ (buffered to pH 4.0) at 80 °C for 3 h. The mixture was washed with deionized water at each step. These treatments were repeated twice. The purified α-chitin powder was freeze-dried and kept in a desiccator before use. The crystallinity of the purified α-chitin powder was 76% by X-ray diffraction. The viscosity-average molecular weight (M_η) of the purified α-chitin powder was determined to be 10.7×10^4 g/mol in a 5 wt% LiCl/dimethylacetamide (DMAc) solution by viscometry at 25 °C [39]. KOH, NaOH, $LiOH\cdot H_2O$, urea, ethanol and *t*-BuOH were purchased from Shanghai Chemical Reagent Co. Ltd., China. All other materials and reagents were used as received.

2.2 Preparation of α-chitin solutions in alkali hydroxide/urea aqueous solutions

The 2.5 M alkali hydroxide (KOH, NaOH and LiOH)/0.67 M urea aqueous solutions were used as solvents for chitin. The purified α-chitin powder in the desired amount was dispersed into alkali hydroxide/urea aqueous solutions to obtain 2 wt%–7 wt% α-chitin suspensions. Subsequently, the suspensions were frozen below −30 °C overnight, and then thawed at 0 °C with stirring. This freeze-thawing procedure was repeated for once, twice and three times, respectively, for KOH/urea, NaOH/urea and LiOH/urea aqueous solutions, in which the α-chitin can be dissolved completely. After removing air bubbles by centrifugation, transparent and viscous α-chitin solutions were achieved. Unless otherwise stated, we mainly focused on α-chitin hydrogels and aerogels at α-chitin concentration of 5 wt%.

2.3 Fabrication of α-chitin hydrogels and aerogels from alkali hydroxide/urea aqueous solutions

The obtained α-chitin solutions were poured into Petri dishes as a 3-mm thick layer or spread on a glass plate as 1-mm thick layer, and then immersed in ethanol for regeneration at 5 °C for 2 h to give α-chitin gels. After thorough washing with deionized water, the α-chitin hydrogels were subjected to solvent-exchange with *t*-BuOH. And then, the α-chitin alcogels were frozen by immersing into liquid nitrogen and subjected to a conventional freezer dryer to achieve α-chitin aerogels.

2.4 Characterization

The dynamic rheology experiment was carried out on an ARES-RFS III rheometer (TA Instruments, USA). A double concentric cylinder geometry with a gap of 2 mm was used to measure dynamic viscoelastic parameters such as the shear storage modulus (G') and loss modulus (G'') as functions of angular frequency (ω) and temperature (T). The rheometer was equipped with two force transducers allowing the torque measurement in the range from 0.004 to 1000 g cm. The values of the strain amplitude were checked to ensure that all measurements were set as 10%, which is within a linear viscoelastic regime. For each measurement, a

fresh α-chitin solution was poured into the couette geometry instrument, which had been kept at each measurement temperature without preshearing or oscillating. Temperature control was established by connection with a Julabo FS18 (China) cooling/heating bath kept within ±0.2 °C over an extended time. A thin layer of low viscosity paraffin oil was spread on the exposed surface of the measured solution to prevent dehydration during rheological measurements. For the frequency sweep measurement, the frequency was from 0.1 to 100 rad/s, and the temperature ranged from −5 to 60 °C. The dynamic temperature sweep measurements were conducted from −5 to 30 °C at an angular frequency of 1 rad/s and with heating rate of 1 °C/min.

Transmission IR absorption spectra of the α-chitin aerogels (pressed into pellets) were acquired with a Fourier transform infrared spectrometer (FT-IR, Perkin Elmer Spectrum, USA) in the region of 400–4000 cm^{-1} with a 2 cm^{-1} resolution and an accumulation of 32 scans.

Morphology of the surface and inner part of the α-chitin aerogels were observed by using a scanning electron microscopy (SEM, Hitachi S-4800, Japan) at an accelerating voltage of 5 kV. Before observation, the sample was coated with golden. The α-chitin alcogels containing *t*-BuOH were frozen in liquid nitrogen and snapped immediately; and then freeze dried.

The X-ray diffractometry (XRD) of the α-chitin aerogels was performed in reflection mode (D8-Advance, Bruker, USA) with CuKα radiation (0.1542 nm) at 40 kV and 30 mA. The samples were mounted on a solid circular holder, and the proportional counter detector was set to collect data at a rate of 1°/min over the 2θ range from 5° to 35°. The peak position and crystallinity were determined by multi-peak fitting of the XRD profiles, and crystallite size were estimated by substituting the full-width at half-maximum (FWHM) into the Scherrer equation.

^{13}C nuclear magnetic resonance (^{13}C NMR) of the α-chitin solutions were carried out on a Bruker DRX-500 spectrometer (Germany) at 5 °C. The sodium salt of 2,2-dimethyl-2-silapentane-5-sulphonic acid (DSS) was used as an internal reference to determine chemical shifts. The α-chitin concentration was about 5 wt%. Cross-polarization/magnetic angle spinning (CP/MAS) solid-state ^{13}C NMR spectra of the α-chitin aerogels were recorded on a Bruker AVANCE-600 spectrometer (Germany) (^{13}C frequency= 150.96 MHz) with a standard 4 mm rotor at ambient temperature. The spin rate was 8.0 kHz. The repetition time and contact time were 4.0 s and 1.0 ms, respectively. ^{13}C chemical shifts were determined from the left signal (38.56 ppm) of adamantine relative to tetramethylsilane. The degree of *N*-acetylation was determined by the ratio of the integration values of the methyl carbon to the anomeric carbon signal [40].

Nitrogen physisorption measurements were performed by a Micromeritics ASAP2020 (USA) at 77 K, and Brunauer-Emmett-Teller (BET) and Barrett-Joyner-Halendar (BJH) analyses were done by software. The α-chitin aerogels were degassed at 105 °C in vaccum to remove all the adsorbed species. The BET analysis was done for relative vapor pressure of 0.05 to 0.3. The BJH analysis was done from the desorption branch of the isotherms.

The porosity ($P_{r,A}$) of the α-chitin aerogels can be calculated by:

$$P_{r,A} = \left(1 - \frac{\rho}{\rho_c}\right) \times 100\%$$

where ρ is the density of the α-chitin aerogel; ρ_c is the density of bulk chitin (1.425 g/cm^3) [41].

Tension and compression tests of the α-chitin hydrogels and aerogels were performed on a universal tensile tester (CMT6503, SANS, China). For the tension measurements, hydrogel and aerogel sheets with 50 mm long, 5 mm wide and 1 mm thickness was stretched at a tension speed of 2 mm/min. The cubic hydrogel and aerogels with 10 mm× 10 mm in length and 3 mm in height was set on the lower plate and compressed by the upper plate at a strain rate of 1 mm/min. The modulus was calculated from the initial linear region of the stress-strain curves.

Thermogravimetry analysis (TGA) for the α-chitin aerogels were performed on a STA 449C thermal analyzer (NETZSCH, Germany) under nitrogen at a heating rate of 10 °C/min from 30 to 600 °C.

Mouse bone mesenchymal stem cells (mBMSCs) were propagated in Dulbecco's Modified Eagle's Medium (DMEM, Gibco, USA) supplemented with 10% fetal bovine serum (FBS, Gibco, USA). Chitin hydrogels were placed in 48-well plates and sterilized in 75% (*v*/*v*) aqueous ethanol solution for 2 h, followed by rinse with sterilized phosphate-buffered saline (PBS) for three times. Subsequently, the hydrogels were pre-wetted with culture medium for 12 h. Then the medium was removed and 500 μL of the mBMSCs suspension with a density of 5×10^3 cells/well was seeded. The cells-seeded hydrogels were incubated at 37 °C in a humidified incubator with 5% CO_2. Cell proliferation on the hydrogels was evaluated by Cell Counting Kit-8 (CCK-8, Dojindo Laboratories, Japan) after 1, 3, 5 and 7 d of culture. In brief, at each time point, the culture medium was removed and the CCK-8 working solution was added to incubate for 1 h at 37 °C. Subsequently, the supernatant medium was extracted and the absorbance at 450 nm was measured by Thermo 3001 microplate reader (Thermo, USA) (n=6). The results were analyzed with one-way analysis of variance (ANOVA) using SPSS 12.0 software (SPSS Inc.; Chicago, IL, USA).

3 Results and discussion

Figure 1 shows the photographs of the α-chitin solutions in aqueous KOH/urea, NaOH/urea and LiOH/urea solutions,

the hydrogels regenerated from ethanol, and the aerogels freeze-dried from *t*-BuOH. Dissolving α-chitin in aqueous alkali hydroxide/urea solutions requires freeze-thawing cycles. After once, twice, and three times of freeze-thawing cycles, respectively, the α-chitin dissolved completely in aqueous KOH/urea, NaOH/urea and LiOH/urea solutions. The chitin in the aqueous KOH/urea and NaOH/urea solutions was clearer than that in the aqueous LiOH/ urea solution (Figure 1(a–c)). In addition, our previous experience suggested that the maximum α-chitin concentration would be 11 wt% in aqueous KOH/urea solution, higher than those in aqueous NaOH/urea (8 wt%) and LiOH/urea (5 wt%). The dissolution of chitin in aqueous KOH/urea solution has not been previously reported. The dissolution mechanism of chitin in aqueous KOH/urea solution will be elucidated in the future. The chitin-dissolution powers of the solvents exhibited the following order: aqueous KOH/urea>NaOH/urea>LiOH/urea. Synthesizing α-chitin hydrogels involves regenerating these chitin solutions through physical gelation with ethanol, followed by thorough washing with deionized water. The chitin hydrogels prepared from aqueous KOH/urea and NaOH/urea solutions were transparent, while that prepared from aqueous LiOH/urea solution was translucent (Figure 1(d)). The resulting chitin hydrogels were subsequently solvent-exchanged with *t*-BuOH and then converted to white aerogels by freeze-drying. The chitin aerogels obtained from aqueous KOH/urea and NaOH/urea solutions were flexible with good mechanical properties, whereas that generated from aqueous LiOH/urea solution was friable and broke easily (Figure 1(e–g)).

The rheological behavior of the α-chitin in aqueous alkali hydroxide/urea solutions was evaluated using a dynamic viscoelastic method. The shear storage modulus (G') at various temperatures as a function of angular frequency (ω) for α-chitin in aqueous KOH/urea, NaOH/urea and LiOH/urea solutions is illustrated in Figure 2. The G' values of all of the α-chitin solutions decreased as the temperature increased from −5 to 5 °C over the entire accessible frequency range, suggesting that the chitin chains were more entangled at low temperatures. Moreover, we also found a positive correlation between G' and $\omega^{1.5}$ at low frequency from −5 to 5 °C, unlike the terminal behavior (G'-ω^2) for a Newtonian fluid [42], possibly because the strong hydrogen bonding interactions in the chitin solutions caused the formation of supramolecular structures [43]. Note that at 20 °C, the G' curves of the α-chitin in aqueous KOH/urea and NaOH/urea solutions present a plateau-like feature at low frequencies, which declines as the frequency increases (Figure 2(a, b)); this behavior suggests that the sol-gel transition occurred and that weak gels were formed. Above 20 °C, the G' curves exhibit an expanded plateau-like behavior as the temperature increases, with significant frequency-independent plateaus over the entire frequency range at 60 °C, indicating the existence of a stable gel network structure [43,44]. In contrast, the α-chitin in aqueous LiOH/urea aqueous solution displays a lower sol-gel transition temperature of 15 °C (Figure 2(c)), probably because of the weaker hydrogen bonding interactions between chitin chains and the aqueous LiOH/urea solution.

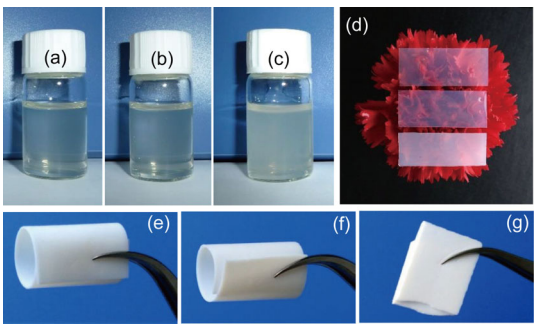

Figure 1 Photographs of α-chitin in KOH/urea (a), NaOH/urea (b) and LiOH/urea (c) solutions after once, twice, and three times of freeze-thawing cycles, respectively. Photographs of the chitin hydrogels (d, from top to bottom) and aerogels (e–g, from left to right) prepared from aqueous KOH/urea, NaOH/urea and LiOH/urea solutions (color online).

We further evaluated the effects of temperature on the G' and G'' values of α-chitin in aqueous alkali hydroxide/urea solutions (Figure 3). Below the gelation temperature, all of the α-chitin solutions were viscous liquids, and their G' values were lower than the G'' values and gradually declined as the temperature increased. When the temperature was close to the gelation temperature, the G'' values continued to decrease slightly, whereas the G' values increased dramatically, suggesting the partial formation of weak chitin gels formed. Above the gelation temperature, all of the α-chitin solutions exhibited temperature-induced rapid gelation behavior. Both the G' and G'' values increased sharply within a very narrow temperature range, and the G' values exhibited a much faster rate of increase than the G'' values, suggesting that the hydrophobic interactions between chitin chains disturbed by heating and the intra- and intermolecular hydrogen bond interactions among the chitin chains strengthened, thereby leading to self-association and chain entanglements [43]. In addition, the gelation temperatures of the α-chitin solutions were 20.0, 21.0 and 15.3 °C based on the crossover temperatures of G' and G'' in aqueous KOH/urea, NaOH/urea and LiOH/urea solutions, respectively. Moreover, the moduli at the gel point were 9.5, 15.4 and 5.3 Pa for α-chitin in KOH/urea, NaOH/urea and LiOH/urea aqueous solutions, respectively. This result confirmed that the chitin chains have stronger intra- and inter-molecular interactions with aqueous KOH/urea and NaOH/urea solutions than with aqueous LiOH/urea solution, resulting in different levels of aggregation and entanglement of the chitin chains.

^{13}C nuclear magnetic resonance (NMR) spectra of these α-chitin solutions are shown in Figure 4. Table 1 summarizes the ^{13}C NMR chemical shifts of α-chitin in various solvents. No chitin derivative peaks appeared in the ^{13}C NMR spectra, suggesting the absence of derivatization and indicating that α-chitin dissolution is a physical process.

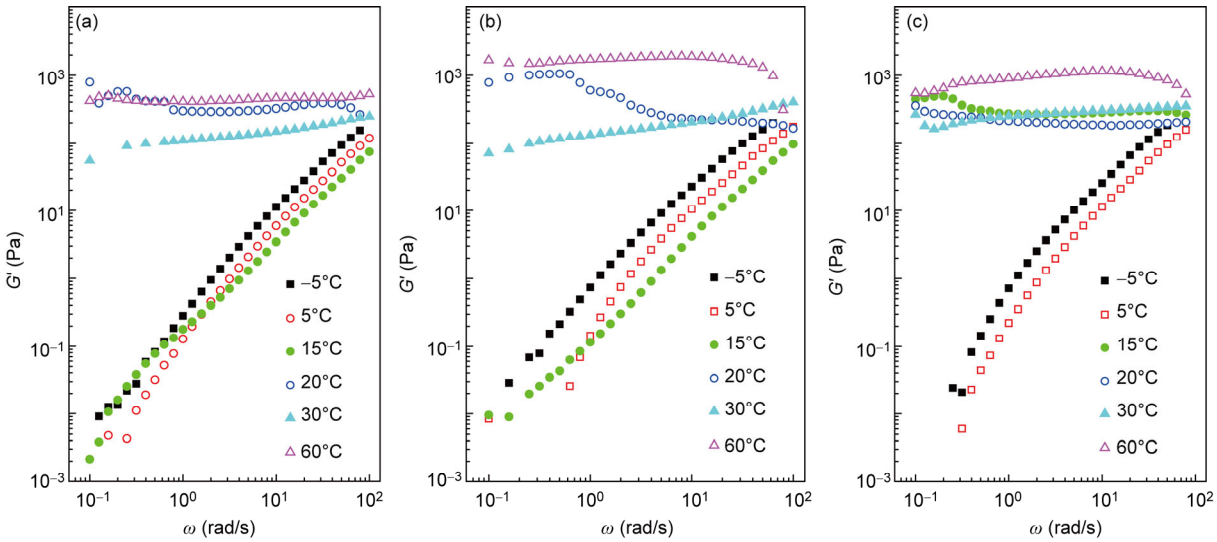

Figure 2 Storage modulus (G') as a function of angular frequency (ω) at various temperatures for α-chitin in aqueous KOH/urea (a), NaOH/urea (b) and LiOH/urea (c) solutions (color online).

Table 1 ^{13}C NMR chemical shifts of the chitin solutions and aerogels

Sample	Solvent	Chemical shift (ppm)								Ref.
		C1	C2	C3	C4	C5	C6	C=O	CH_3	
Solution	LiOH/urea/D_2O	100.6	55.3	71.7	78.9	75.3	59.8	173.8	21.5	This work
	NaOH/urea/D_2O	100.6	55.3	71.7	78.7	75.7	59.8	173.8	21.7	This work
	KOH/urea/D_2O	100.5	55.3	71.7	78.7	75.7	59.8	173.8	21.8	This work
	LiSCN	103.8	58.3	74.8	80.7	74.8	61.7	174.4 [a)]	22.0 [a)]	[17]
	LiCl/DMAc	102.1	55.7	74.5	80.5	76.2	59.1	–	–	[17]
Aerogel	LiOH/urea/D_2O	104.5	55.4	73.7	83.2	76.1	61.2	173.6	23.1	This work
	NaOH/urea/D_2O	104.4	55.4	73.7	83.5	76.0	61.3	173.8	23.1	This work
	KOH/urea/D_2O	104.3	55.5	73.7	83.3	75.9	61.2	173.7	23.1	This work

a) Data of chitobiose in D_2O.

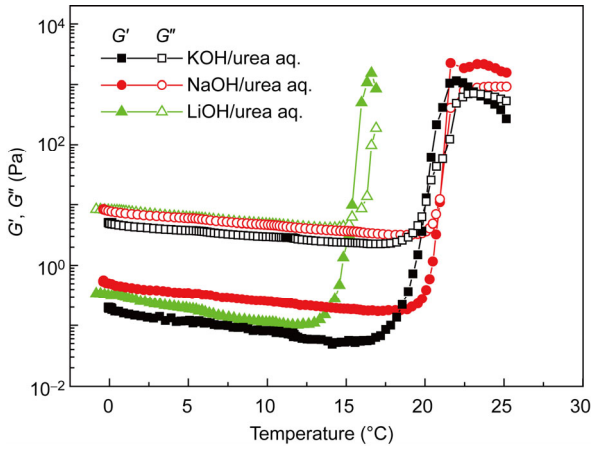

Figure 3 Temperature dependence of the storage modulus (G') and the loss modulus (G'') for α-chitin in aqueous KOH/urea, NaOH/urea and LiOH/urea solutions (color online).

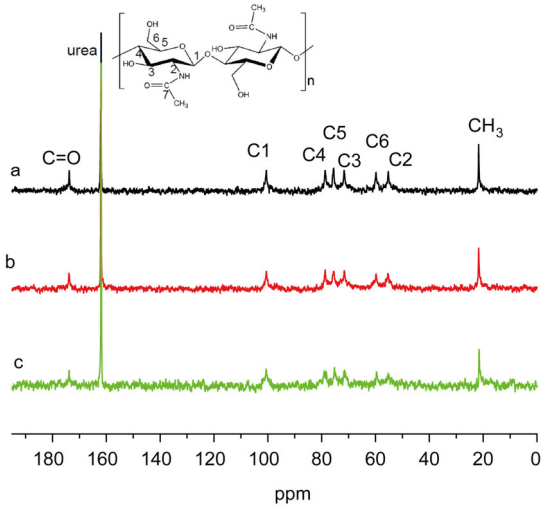

Figure 4 ^{13}C NMR spectra of α-chitin in KOH/urea/D_2O (a), NaOH/urea/D_2O (b) and LiOH/urea/D_2O (c) (color online).

Moreover, the ^{13}C NMR chemical shifts of C=O (173.8 ppm), C1 (100.5–100.6 ppm), C4 (78.7–78.9 ppm), C5 (75.3–75.7 ppm), C3 (71.7 ppm), C6 (59.8 ppm), C2 (55.3 ppm) and CH_3 (21.5–21.8 ppm) were very close, indicating that α-chitin has similar chain conformations in aqueous alkali hydroxide/urea solutions. Thus, these aqueous alkali hydroxide/urea solutions are non-derivatizing solvents for α-chitin, and real chitin solutions can be produced by freeze-thawing cycles.

The Fourier transform infrared (FT-IR) spectra of all of the chitin aerogels were characteristic of α-chitin (Figure 5). The chitin aerogels exhibited peaks at 1660 cm^{-1} with a slight shoulder at 1624 cm^{-1} corresponding to the amide I bands of α-chitin: stretching of C=O groups hydrogen bonded to NH groups of neighboring chitin chains and stretching of C=O groups hydrogen bonded to both NH and C(6)–OH groups on the same chain, respectively [45–47]. The relative intensity of the amide bands increased and the width of the O–H stretching peak (3000 to 3740 cm^{-1}) narrowed from aqueous LiOH/urea to KOH/urea, suggesting that the hydrogen bonding interactions in chitin aerogels strengthened.

The XRD diffraction patterns of the chitin aerogels are shown in Figure 6. All the chitin aerogels show six characteristic crystalline diffraction peaks at 9.3°, 12.8°, 19.3°, 20.7°, 23.4° and 26.4° in the 2θ range from 5° to 35°; these peaks were ascribed to the (020), (021), (110), (120), (130) and (013) reflections, respectively, of a typical α-chitin crystal [45,48]. Note that the FWHM of the reflections increased with the atomic number of the alkali metal. However, the intensity of the reflections decreased, and the (120) and (130) reflections were much weaker in chitin aerogels prepared from aqueous KOH/urea and NaOH/urea solutions. By peak fitting the diffraction profiles, the crystallinities of the chitin aerogels were calculated to be 53%, 63% and 66% when prepared from aqueous KOH/urea, NaOH/urea and LiOH/urea solutions, respectively. These results indicate that despite its low crystallinity, α-chitin has a stable aggregate structure after undergoing dissolution and regeneration.

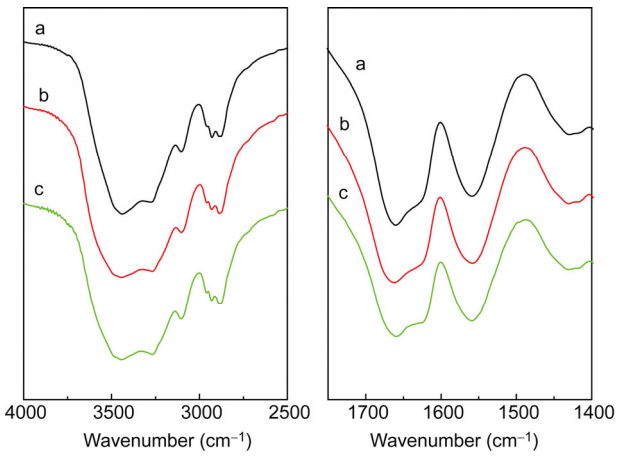

Figure 5 FT-IR spectra of the α-chitin aerogels prepared from aqueous KOH/urea (a), NaOH/urea (b) and LiOH/urea (c) solutions.

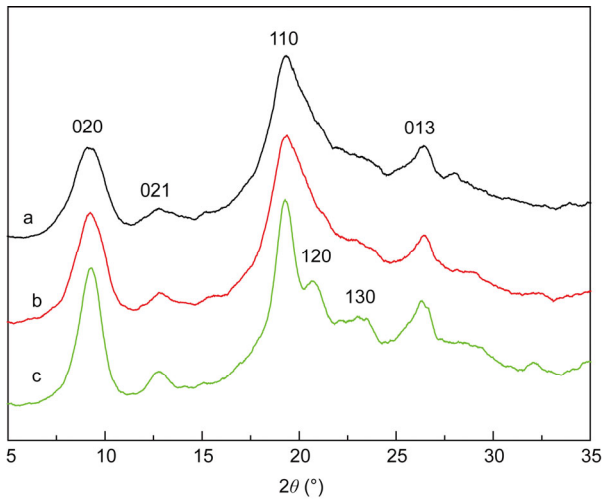

Figure 6 X-ray diffraction (XRD) profiles of the α-chitin aerogels prepared from aqueous KOH/urea (a), NaOH/urea (b) and LiOH/urea (c) solutions.

Further evidence of the crystalline phase and the hydrogen bonding interactions was obtained via ^{13}C NMR. Figure 7 shows the cross-polarization magic angle spinning (CP/MAS) ^{13}C NMR spectra of the α-chitin aerogels prepared from aqueous KOH/urea, NaOH/urea and LiOH/urea solutions. The degrees of the *N*-acetylation of these α-chitin aerogels were evaluated based on the ^{13}C NMR spectra: 93%, 89% and 87% from aqueous KOH/urea, NaOH/urea and LiOH/urea solutions, respectively. The ^{13}C NMR chemical shifts of C=O (173.6–173.8 ppm), C1 (104.3–104.5 ppm), C4 (83.2–83.5 ppm), C5 (75.9–76.1 ppm), C3 (73.7 ppm), C6 (61.2–61.3 ppm), C2 (55.4–55.5 ppm) and CH_3 (23.1 ppm) for α-chitin aerogels are listed in Table 1. The chemical shift values for all of the α-chitin aerogels were consistent with previously reported values for α-chitin [46,49,50]. The line width of the asymmetric broad peak of C=O carbon was composed of two peaks, which were

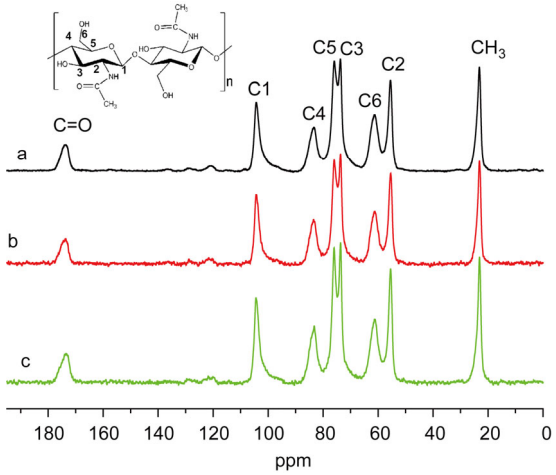

Figure 7 The CP/MAS ^{13}C NMR spectra of α-chitin aerogels prepared from aqueous KOH/urea (a), NaOH/urea (b) and LiOH/urea (c) solutions.

closely related to two types of hydrogen bonds (as observed in the FT-IR spectra) that account for the splitting of the amide I band [47,51,52]. The width of the carbonyl peak becomes narrower from aqueous LiOH/urea to KOH/urea solutions, suggesting that the hydrogen bonding interactions in α-chitin aerogels strengthen. In addition, C3 and C5 appeared as two signals, which is characteristic of α-chitin, while the degree of splitting of the two peaks decreased from aqueous LiOH/urea to KOH/urea solutions; this is attributed to decreased crystallinity and increased hydrogen bonding interactions in the α-chitin aerogels [49,50,53].

All of these α-chitin aerogels exhibit highly open porosity consisting of nanofibrils with diameters of less than 50 nm (Figure 8). However, these aerogels showed different morphologies and pore structures. The α-chitin aerogel prepared from aqueous LiOH/urea had a micrometer- and nanometer-sized heterogeneous pore structure composed of loose aggregates of chitin nanofibrils (Figure 8(a, d)). In contrast, those prepared from aqueous NaOH/urea (Figure 8(b, e)) and KOH/urea (Figure 8(c, f)) solutions comprised percolating nanofibrillar networks with relatively uniform, nanometer-sized pore structures. These differences likely result from differences in the chitin-regeneration conditions; that is, LiOH is insoluble in the coagulant and undergoes rapid coagulation to form large precipitates in chitin gels, whereas NaOH and KOH are soluble in the coagulant and experience gradual liquid exchange from the chitin solution to the coagulant and spontaneous self-assembly of chitin nanofibrils.

The nitrogen adsorption isotherms for all of the α-chitin aerogels were of IUPAC (International Union of Pure and Applied Chemistry) type IV, that is, multilayer adsorption onto a mesoporous solid with strong adsorbent-adsorbate interactions (Figure 9). In terms of the specific surface area,

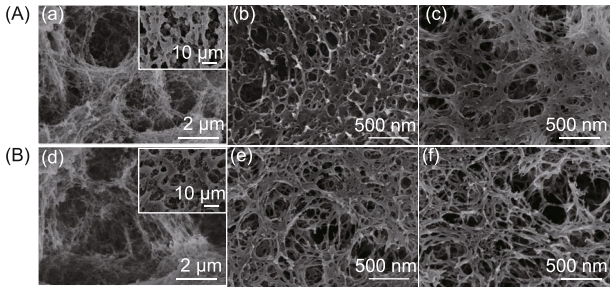

Figure 8 Scanning electron microscopy (SEM) images of the surface (A) and inner part (B) of the α-chitin aerogels prepared from aqueous LiOH/urea (a, d), NaOH/urea (b, e) and KOH/urea (c, f) solutions. The insets show low-magnification SEM images.

aqueous KOH/urea solution exhibit fairly good performance as a solvent for aerogel fabrication (485 m^2/g vs. 346 and 352 m^2/g) (Table 2). The porosity of these α-chitin aerogels ranged from 87% to 94%. The most probable values of the mesopore diameter were between 10 and 90 nm. However, decreasing the chitin concentration in aqueous KOH/urea solution had a remarkable influence on the aerogel structure. The density of the α-chitin aerogels decreased from 0.19 to 0.09 g/cm^3, whereas the specific surface area and pore volume increased from 419 to 535 m^2/g and from 2.7 to 3.8 cm^3/g, respectively.

These α-chitin aerogels also exhibited excellent mechanical performance that was far superior to those of chitin aerogels prepared from LiCl/DMAc [54], 1-butyl-3-imidazolium acetate [55], and chitin nanowisker/nanofibril suspension [56,57]. To investigate the mechanical properties of these α-chitin hydrogels and aerogels, we evaluated their stress-strain curves under stretching and compression mod els (Figure 10). The tensile strength and modulus of the

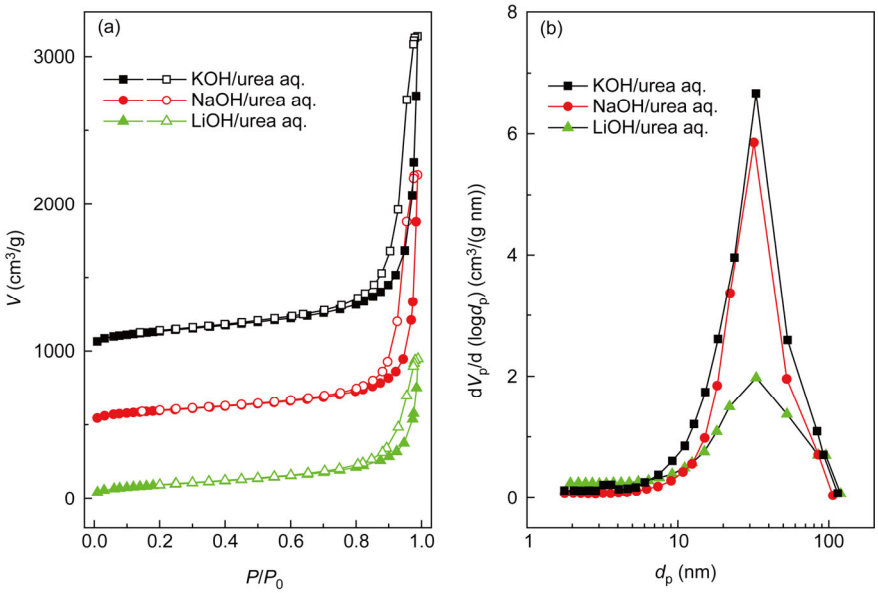

Figure 9 Nitrogen adsorption and desorption isotherms (a) and Barrett-Joyner-Halenda (BJH) pore size distributions (b) (calculated from the desorption branch of the isotherm; d_p=pore diameter, and V_p=pore volume) of the α-chitin aerogels prepared from aqueous KOH/urea, NaOH/urea and LiOH/urea solutions (color online).

Table 2 Physical properties of the α-chitin hydrogels and aerogels

Solvent	C [a] (wt%)	Hydrogel					Aerogel					
		W_{H_2O} [b] (%)	σ [c] (MPa)	ε [c] (%)	E [c] (MPa)	$P_{r,A}$ [b] (%)	ρ (g/cm^3)	S_{BET} [d] (m^2/g)	V [e] (cm^3/g)	$2r$ [e] (nm)	σ* [c] (MPa)	E [c] (MPa)
LiOH/urea/ H_2O	5	94	0.6	70	0.39	94	0.09	346	1.5	17	0.7	1.8
NaOH/urea/ H_2O	5	90	1.2	63	0.15	88	0.17	352	2.6	30	4.4	2.7
KOH/urea/ H_2O	2	94	0.2	58	0.03	94	0.09	535	3.8	28	1.2	0.3
	3	92	0.4	63	0.08	92	0.11	515	3.7	29	2.4	0.7
	4	90	0.6	65	0.21	90	0.14	481	3.4	29	3.1	4.1
	5	91	0.9	61	0.11	89	0.15	485	3.3	27	3.5	2.6
	6	89	1.4	63	0.13	88	0.17	451	3.1	27	6.0	2.3
	7	87	1.7	62	0.25	87	0.19	419	2.7	26	7.1	3.2

a) C is the chitin concentration; b) W_{H_2O} and $P_{r,A}$ are the water content and porosity, respectively, of the hydrogels and aerogels; c) σ, σ*, ε and E are the fracture stress, stress at 60% strain, fracture strain and elastic modulus, respectively, of the gels under the compressive model; d) S_{BET} is the BET surface area at a relative vapor pressure of 0.05–0.3 at 77 K; e) V and $2r$ are the pore volumes determined at a P/P_0 of 0.99 and the average pore diameter of aerogels determined by the BJH method, respectively.

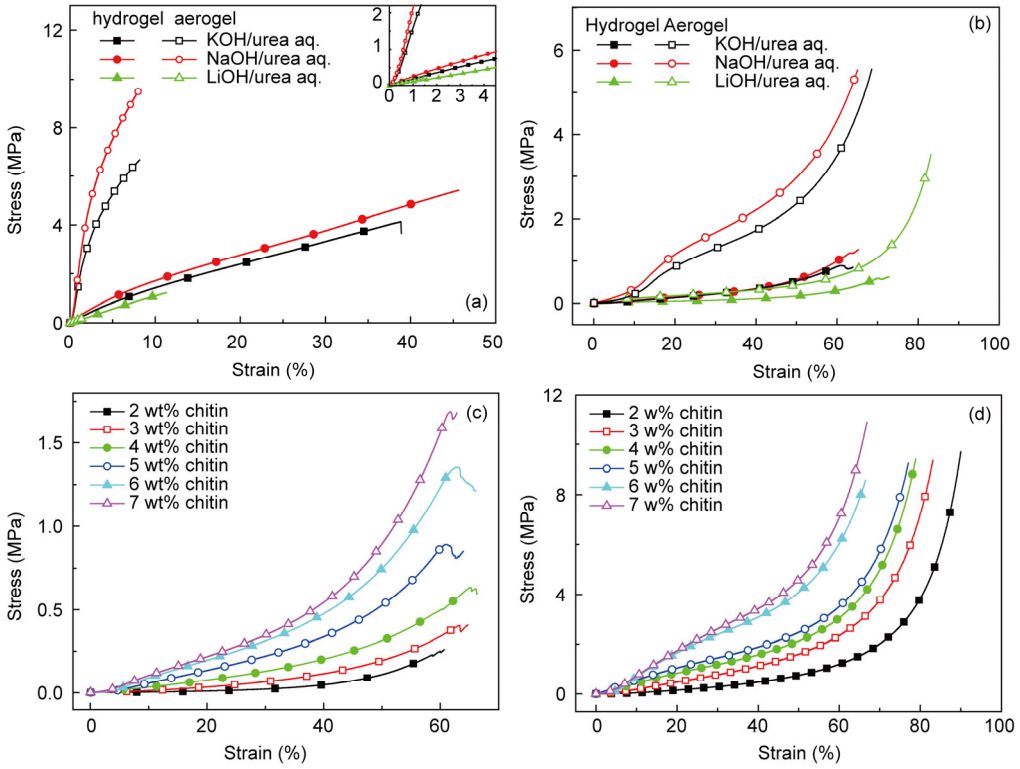

Figure 10 Stress-strain curves of the α-chitin hydrogels (filled) and aerogels (open) prepared from 5 wt% chitin in KOH/urea, NaOH/urea and LiOH/urea aqueous solutions under the tension (a) and compression (b) models. Compressive stress-strain curves of the chitin hydrogels (c) and aerogels (d) in a chitin concentration series prepared from KOH/urea aqueous solution. Inset is the stress-strain curves of the α-chitin hydrogels and aerogels at low strain (color online).

α-chitin hydrogels under the stretching model were determined to be 4.1 and 19.2 MPa, 5.4 and 24.8 MPa, and 1.2 and 10.5 MPa, respectively, for the hydrogels prepared from aqueous KOH/urea, NaOH/urea and LiOH/urea solutions, respectively (Figure 10(a)). After freeze-drying from *t*-BuOH, the α-chitin aerogel prepared from aqueous LiOH/

urea solution had relatively poor mechanical properties and broke easily (tensile strength, 0.2 MPa; Young's modulus, 13.3 MPa). In contrast, those prepared from aqueous NaOH/urea and KOH urea solutions exhibited much stronger mechanical properties, as evidenced by their higher tensile strength values (9.6 and 6.7 MPa, respectively) and Young's moduli (80.5 and 60.7 MPa, respectively).

The compression behaviors of the α-chitin hydrogels and aerogels showed obvious differences between solvents. Compared with the α-chitin hydrogels and aerogels prepared from aqueous LiOH/urea solution, those prepared from aqueous NaOH/urea and KOH/urea solutions were much stronger (Figure 10(b), Table 2). Moreover, the viscosity-average molecular weights (M_η) of these chitin aerogels were ranging from 9.4×10^4 to 9.9×10^4 g/mol. Thus, this difference resulted from the micrometer- and nanometer-sized heterogeneous pore structure composed of loose aggregates of chitin nanofibrils of the α-chitin gels prepared from aqueous LiOH/urea solution versus the uniform nanometer-sized pore structure of self-assembled chitin nanofibrils of those prepared from aqueous NaOH/urea and KOH/urea solutions.

We also performed compression tests to evaluate the mechanical properties of the α-chitin hydrogels and aerogels prepared from aqueous KOH/urea solution using different chitin concentrations. The fracture strain of the α-chitin hydrogels was ca. 63%, regardless of the chitin concentration, whereas when the chitin concentration was increased from 2 wt% to 7 wt%, the compressive stress values and moduli of the α-chitin hydrogels and aerogels increased gradually. For example, the maximum compressive stress values and elastic moduli of the α-chitin hydrogels increased from 0.2 to 1.7 MPa and 0.03 to 0.25 MPa (Figure 10(c)), respectively. Additionally, the compressive stress values (at a strain of 60%) and elastic moduli of the α-chitin aerogels increased from 1.2 to 7.0 MPa and 0.3 to 3.2 MPa, respectively (Figure 10(d)). The thermogravimetric (TG) and derivative TG (DTG) curves of all of the α-chitin aerogels indicated very similar thermal decomposition events at 250 to 350 °C in air (see Figure S1 in the Supporting Information online), suggesting moderate thermal stability.

The hydrophilicity of the chitin aerogels allows the absorbance of aqueous liquids upon rewetting. The proliferation and viability of mBMSCs cultured on the hydrogels were studied *in vitro* (Figure 11). The high porosity of chitin hydrogels could offer analogous environments for extracellular matrix that is conductive to cell adhesion and proliferation. Interestingly, significant differences were observed among these chitin hydrogels after 5 d. The proliferation rate of mBMSCs on the surface of chitin hydrogels from aqueous KOH/urea and NaOH/urea were superior to the chitin aerogel from aqueous LiOH/urea. Mainly because the mesh size and mechanical properties of the hydrogels from aqueous KOH/urea and NaOH/urea are in favour of cell adhesion and proliferation, indicating preferable biocompatibility and potential application for tissue engineering.

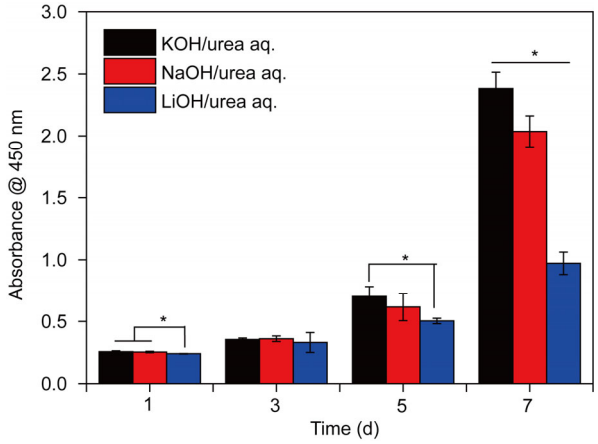

Figure 11 Proliferation of mBMSCs cultured on the surface of σ-chitin hydrogels prepared from aqueous KOH/urea, NaOH/urea and LiOH/urea solutions, respectively (color online).

4 Conclusions

In summary, for the first time, we report that α-chitin can be dissolved in aqueous KOH/urea solution via a freeze-thawing cycle. Moreover, the dissolution powers of the aqueous alkali hydroxide/urea solvents for α-chitin exhibited the following order: aqueous KOH/urea>NaOH/urea>LiOH/urea. All of the α-chitin solutions exhibited temperature-induced rapid gelation behavior. The aqueous alkali hydroxide/urea solutions were shown to be non-derivatizing solvents for α-chitin. Nanostructured α-chitin hydrogels and aerogels were fabricated by regenerating the chitin solutions in ethanol, followed by freeze-drying from *t*-BuOH. The α-chitin aerogels exhibited high porosity, low density, high specific surface area and large pore volume. Additionally, the α-chitin aerogels exhibited good mechanical properties under tension and compression models. *In vitro* studies show that mBMSCs cultured on chitin hydrogels have good biocompatibility. The simplicity of the process and the nanostructured α-chitin aerogels produced may be useful for biomedical materials.

Acknowledgments This work was supported by the National Natural Science Foundation of China (21422405, 51373125) and the Major Program of National Natural Science Foundation of China (21334005). The authors thank to the facility support of the Natural Science Foundation of Hubei Province and the Fundamental Research Funds for the Central Universities.

Conflict of interest The authors declare that they have no conflict of interest.

Supporting information The supporting information is available online at http://chem.scichina.com and http://link.springer.com/journal/11426. The supporting materials are published as submitted, without typesetting or editing. The responsibility for scientific accuracy and content remains entirely with the authors.

1 Nair LS, Laurencin CT. *Prog Polym Sci*, 2007, 32: 762–798
2 Wang S, Lu A, Zhang LN. *Prog Polym Sci*, 2016, 53: 169–206
3 Bartlett DH, Azam F. *Science*, 2005, 310: 1775–1777
4 Wan ACA, Tai BCU. *Biotechnol Adv*, 2013, 31: 1776–1785
5 Arun KR, Sivashanmugam A, Deepthi S, Iseki S, Chennazhi KP, Nair SV, Jayakumar R. *ACS Appl Mater Interf*, 2015, 7: 9399–9409
6 Rinaudo M. *Prog Polym Sci*, 2006, 31: 603–632
7 Liu XX, Wang YF, Zhang NZ, Shanks RA, Liu HS, Tong Z, Chen L. *Chin J Polym Sci*, 2014, 32: 108–114
8 Yu YY, Guo L, Wang W, Wu J, Yuan Z. *Sci China Chem*, 2015, 58: 1866–1874
9 Pillai C, Paul W, Sharma CP. *Prog Polym Sci*, 2009, 34: 641–678
10 Yan N, Chen X. *Nature*, 2015, 524: 155–157
11 Ifuku S, Saimoto H. *Nanoscale*, 2012, 4: 3308–3318
12 Austin PR. Solvents for and purification of chitin. US Patent, 3892731. 1975-07-01
13 Sannan T, Kurita K, Iwakura Y. *Die Makromolekulare Chemie*, 1975, 176: 1191–1195
14 Feng F, Liu Y, Hu K. *Carbohyd Res*, 2004, 339: 2321–2324
15 Einbu A, Naess SN, Elgsaeter A, Vårum KM. *Biomacromolecules*, 2004, 5: 2048–2054
16 Tamura H, Nagahama H, Tokura S. *Cellulose*, 2006, 13: 357–364
17 Gagnaire D, Germain JS, Vincendon M. *Die Makromolekulare Chemie*, 1982, 183: 593–601
18 Kumar MNR. *React Funct Polym*, 2000, 46: 1–27
19 Xie H, Zhang S, Li S. *Green Chem*, 2006, 8: 630–633
20 Wu Y, Sasaki T, Irie S, Sakurai K. *Polymer*, 2008, 49: 2321–2327
21 Qin Y, Lu X, Sun N, Rogers RD. *Green Chem*, 2010, 12: 968–971
22 Sharma M, Mukesh C, Mondal D, Prasad K. *RSC Adv*, 2013, 3: 18149–18155
23 Mukesh C, Mondal D, Sharma M, Prasad K. *Carbohyd Polym*, 2014, 103: 466–471
24 Ladet S, David L, Domard A. *Nature*, 2008, 452: 76–79
25 Shi Z, Gao H, Feng J, Ding B, Cao X, Kuga S, Wang Y, Zhang L, Cai J. *Angew Chem Int Ed*, 2014, 53: 5380–5384
26 Torres JG, Femmer T, Laporte LD, Tigges T, Rahimi K, Gremse F, Zafarnia F, Lederle W, Ifuku S, Wessling M. *Adv Mater*, 2015, 27: 2989–2995
27 Rejinold SN, Chennazhi KP, Tamura H, Nair SV, Rangasamy J. *ACS Appl Mater Interf*, 2011, 3: 3654–3665
28 Shen X, Shamshina JL, Berton P, Gurau G, Rogers RD. *Green Chem*, 2016, 18: 53–75
29 Cai J, Zhang L. *Macromol Biosci*, 2005, 5: 539–548
30 Hu X, Du Y, Tang Y, Wang Q, Feng T, Yang J, Kennedy JF. *Carbohyd Polym*, 2007, 70: 451–458
31 Chang C, Chen S, Zhang L. *J Mater Chem*, 2011, 21: 3865–3871
32 Fan M, Hu Q. *Carbohyd Res*, 2009, 344: 944–947
33 Ding B, Cai J, Huang J, Zhang L, Chen Y, Shi X, Du Y, Kuga S. *J Mater Chem*, 2012, 22: 5801–5809
34 Duan B, Gao H, He M, Zhang L. *ACS Appl Mater Interf*, 2014, 6: 19933–19942
35 Huang Y, Zhong Z, Duan B, Zhang L, Yang Z, Wang Y, Ye Q. *J Mater Chem B*, 2014, 2: 3427–3432
36 Duan B, Zheng X, Xia Z, Fan X, Guo L, Liu J, Wang Y, Ye Q, Zhang L. *Angew Chem Int Ed*, 2015, 54: 1–6
37 Fang Y, Duan B, Lu A, Liu M, Liu H, Xu X, Zhang L. *Biomacromolecules*, 2015, 16: 1410–1417
38 Cai J, Huang J, Zhang L. Solvent compounds for chitin dissolution. China Patent, 201310034088.4. 2013-04-24
39 Terbojevich M, Carraro C, Cosani A, Marsano E. *Carbohyd Res*, 1988, 180: 73–86
40 Heux L, Brugnerotto J, Desbrières J, Versali MF, Rinaudo M. *Biomacromolecules*, 2000, 1: 746–751
41 Okuyama K, Noguchi K, Miyazawa T, Yui T, Ogawa K. *Macromolecules*, 1997, 30: 5849–5855
42 Nijenhuis KT, Winter HH. *Macromolecules*, 1989, 22: 411–414
43 Cai J, Zhang L. *Biomacromolecules*, 2006, 7: 183–189
44 Arvidson S, Lott J, McAllister J, Zhang J, Bates F, Lodge T, Sammler R, Li Y. *Macromolecules*, 2012, 46: 300–309
45 Minke R, Blackwell J. *J Mol Biol*, 1978, 120: 167–181
46 Focher B, Naggi A, Torri G, Cosani A, Terbojevich M. *Carbohyd Polym*, 1992, 17: 97–102
47 Sikorski P, Hori R, Wada M. *Biomacromolecules*, 2009, 10: 1100–1105
48 Ogawa Y, Kimura S, Wada M, Kuga S. *J Struct Biol*, 2010, 171: 111–116
49 Tanner SF, Chanzy H, Vincendon M, Roux JC, Gaill F. *Macromolecules*, 1990, 23: 3576–3583
50 Cárdenas G, Cabrera G, Taboada E, Miranda SP. *J Appl Polym Sci*, 2004, 93: 1876–1885
51 Kameda T, Miyazawa M, Ono H, Yoshida M. *Macromol Biosci*, 2005, 5: 103–106
52 Brugnerotto J, Lizardi J, Goycoolea F, Argüelles-Monal W, Desbrieres J, Rinaudo M. *Polymer*, 2001, 42: 3569–3580
53 Massiot D, Touzo B, Trumeau D, Coutures J, Virlet J, Florian P, Grandinetti P. *Solid State Nucl Mag*, 1996, 6: 73–83
54 Tsioptsias C, Michailof C, Stauropoulos G, Panayiotou C. *Carbohydr Polym*, 2009, 76: 535–540
55 Silva SS, Duarte ARC, Carvalho AP, Mano JF, Reis RL. *Acta Biomaterialia*, 2011, 7: 1166–1172
56 Heath L, Zhu L, Thielemans W. *ChemSusChem*, 2013, 6: 537–544
57 Tsutsumi Y, Koga H, Qi ZD, Saito T, Isogai A. *Biomacromolecules*, 2014, 15: 4314–4319